Ciesielski, P. F., Kristoffersen, Y., et al., 1991
Proceedings of the Ocean Drilling Program, Scientific Results, Vol. 114

40. GEOCHEMICAL INVESTIGATIONS OF VOLCANIC ASH LAYERS FROM SOUTHERN ATLANTIC LEGS 113 AND 114[1]

Hans-W. Hubberten,[2] Wolfgang Morche,[2] Frances Westall,[2] Dieter K. Fütterer,[2] and Jörg Keller[3]

ABSTRACT

Petrographic and geochemical investigations were carried out on 21 ash layers from four sites of ODP Legs 113 and 114 in the southern Atlantic Ocean. With the help of geochemical data and petrographic characterization three rock series can be distinguished for stratigraphically different ash layers from Site 701 (Leg 114) located east of the South Sandwich Island Arc, whereas the Leg 113 tephras from the southern slope of the South Orkney Microcontinent belong to another magmatic series. Geochemical correlation of the Leg 113 tephras with possible source areas indicates that they were probably erupted from the Antarctic Peninsula.

The Miocene ashes from Site 701 are probably derived from the now-extinct Discovery Arc, the precursor of the South Sandwich Islands. The Pliocene ashes from the site show some affinity with the South Shetland Islands, although the available data do not permit a clear correlation. The Quaternary ashes from Site 701 display a chemistry typical of island-arc tholeiites and are therefore most probably derived from eruptions on the South Sandwich Islands. Because of their distant position the southern Andes seem to be rather improbable as a potential source region for the tephra layers investigated.

INTRODUCTION

Eight holes from four Ocean Drilling Program (ODP) drill sites in the western Antarctic–South Atlantic Ocean were selected for studies of volcanic ash geochemistry. Holes 695A, 696A, 696B, 697A, and 697B from ODP Leg 113 are located between 40° and 44°W and 61° and 63°S on the southwestern slope of the South Orkney Microcontinent (Fig. 1; Barker, Kennett, et al., 1988). The large number of green, devitrified volcanic ash layers—in addition to several thin (<5 cm) discrete layers of unaltered volcanic glass—found in the Pliocene sediments in these holes reflects the influence of numerous volcanic eruptions. The Leg 114 samples come from Site 701, located at 51°59.07′S, 23°12.73′W (Fig. 1; Ciesielski, Kristoffersen, et al., 1988). The ash layers encountered at this site range in thickness from 2 to 10 cm and occur in lower Miocene to Quaternary sediments. Thin layers of green, altered ash are also common at Site 701.

In accordance with the prevailing westerly winds in this region, the search for source areas of the tephras (distributed by wind, ocean currents, and/or sea ice rafting) was to the west of the sites drilled.

The purpose of this study is to describe the textures and the chemical composition of the ash layers containing fresh volcanic glass. With the help of these data, the provenance of the volcanic material will be discussed. During the time span examined (Miocene to the present), volcanic activity in the vicinity of the drill sites is recorded from the Antarctic Peninsula, South Shetland Islands, and the South Sandwich Islands and their precursor, the Discovery Arc (Fig. 1).

The magmas erupted in this area can be characterized as a subduction-related calc-alkaline series (Miocene-Pliocene in the Antarctic Peninsula and, to a certain extent, the South Shetland Islands), changing to alkali-enriched compositions associated with backarc spreading during the Quaternary (South Shetland Islands, Bransfield Strait volcanics, and Seal Nunataks) (Dalziel, 1983; Gonzalez-Ferran, 1982; Keller et al., 1988; Saunders et al., 1980; Smellie, 1983; Smellie et al., 1984, 1988; Tarney et al., 1982; Weaver et al., 1979, 1982). In contrast, the intraoceanic South Sandwich Islands (Pliocene-Pleistocene) and their inferred precursors (the late Miocene Discovery Arc and Jane Bank) exhibit less evolved magma series of the island-arc tholeiitic type with a transition to calc-alkaline compositions (Baker, 1978; Barker et al., 1982).

Previous investigations of young tephra layers from this region by Ninkovich et al. (1964), Federman et al. (1982), and Smith et al. (1983) covered the last 150,000 yr of sedimentation. Numerous tephra layers that originated from the South Sandwich Islands have been recorded, with at least one major eruption at about 30,000 yr ago (Federman et al., 1982). Smith et al. (1983) postulated tephra deposition from South Sandwich eruptions by ice rafting as far as 13°E and 46°S.

MATERIALS AND METHODS

For this geochemical study of volcanic ash a total of 22 samples from Leg 113 was investigated. Seven samples were taken aboard ship and the rest were obtained by additional sampling at the core repository. The latter were selected from apparent ash horizons on the basis of the visual core descriptions, but in only a few cases did the samples actually contain abundant glass shards (Table 1). Volcanic ash is a common minor constituent in the sediments at Sites 696 and 697, although in Hole 695A it has some occurrences as a major constituent and is found either generally disseminated throughout the sediment or in patchy concentrations in burrows. Well-defined ash layers are rare in the Leg 113 sediments. Only two ash layers are thicker than 3 cm. All the investigated layers are of Pliocene age (Fig. 2).

Nine samples from 30 visible ash layers in the three holes drilled at Site 701 were analyzed (Table 1). The samples were taken aboard ship and all are from discrete ash layers. Four ash layers from upper Pliocene to Quaternary sediments were investigated from Hole 701A, whereas the ashes studied from

[1] Ciesielski, P. F., Kristoffersen, Y., et al., 1991. *Proc. ODP, Sci. Results*, 114: College Station, TX (Ocean Drilling Program).

[2] Alfred-Wegener-Institute for Polar and Marine Research, Columbusstraße, D-2850 Bremerhaven, FRG (Westall, present address: Université de Nantes, Laboratoire de Biosédimentologie, Sciences de la Terre, 2, Chemin de la Houssinière, F-44072 Nantes, France).

[3] Mineralogisch-Petrographisches Institut, Universität Freiburg/Br., Albertstr. 23b, D-7800 Freiburg, FRG.

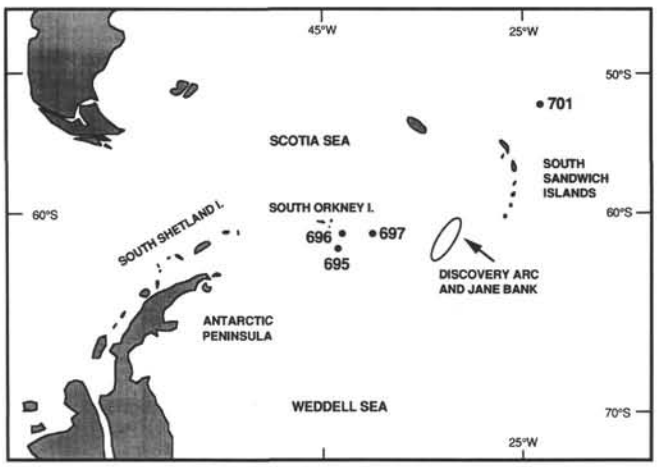

Figure 1. Principal source regions for pyroclastic products in the southwestern Atlantic Ocean. Ash-bearing sediments were investigated from ODP Sites 695, 696, and 697 of Leg 113 and Site 701 of Leg 114.

the lower Pliocene were sampled in Hole 701B. The one lower Miocene and two upper Miocene ash layers from Hole 701C represent the oldest volcanic products analyzed in this investigation (Fig. 2).

The examined samples are identified by Alfred-Wegener-Institute (AWI) laboratory sample numbers corresponding to ODP sample designations (Table 1).

All samples were dried at 50°C and weighed. Carbonate was removed by adding 10% hydrochloric acid. The carbonate-free residue was rinsed with distilled water, dried, and reweighed. The samples were then sieved in order to obtain <63-, 63–200-, and >200-μm fractions. Only the 63–200-μm fraction was investigated.

The samples were described using a petrographic microscope. Special textural phenomena were documented with help of a scanning electron microscope (SEM). The glass shards were separated using heavy liquids and a Frantz Isodynamic magnetic separator, with the magnetic field strength varied to obtain the different glass fractions.

Polished grain mounts were prepared from the separated volcanic glasses and minerals of each ash layer for microprobe analyses and petrographic investigations. Geochemical analysis was performed with energy-dispersive KEVEX equipment (EDX) attached to an SEM at Freiburg University using the method described by Morche (1988). To avoid uncontrolled loss of Na_2O, glass particles were measured under a defocused electron beam of 10 × 10 μm minimum size (accelerating voltage 15 kV, beam current approximately 5 nA, and count-

Table 1. Investigated ash layers from ODP Legs 113 and 114.

Age	Sample (Core, section, interval in cm)	AWI sample designation	Thickness of ash layer (cm)	Chemical analysis
	114-701A-			
Quaternary	1H-4, 58–60	1–1	7	Yes
Quaternary	2H-4, 17–18	1–2	7	Yes
Quaternary	5H-5, 58–59	2	4	Yes
late Pliocene	8H-4, 55–56	3	2	Yes
	114-701B-			
early Pliocene	3H-4, 84–86	4	10	Yes
early Pliocene	4H-1, 132–134	5	7	Yes
	114-701C-			
late Miocene	24H-7, 13–15	6	3	Yes
late Miocene	25X-1, 143–145	7	6	Yes
early Miocene	37X-1, 126–128	8	4	Yes
	113-696A-			
late Pliocene	7H-3, 5–7	16	Disseminated	Yes
late Pliocene	7H-7, 53–55	17	2	Yes
late Pliocene	9H-2, 4–6	18	1	Yes
	113-695A-			
early Pliocene	1H-1, 50–51		No glass	No
early Pliocene	9H-2, 5–7	9	5	Yes
early Pliocene	14H-CC, 34–36		No glass	No
early Pliocene	18X-4, 120–121	10	4	Yes
early Pliocene	21X-2, 68–70	11	1	Yes
early Pliocene	23X-5, 61–63	12	2	Yes
early Pliocene	25X-1, 89–91	14	3	Yes
early Pliocene	25X-6, 3–5	13	2	Yes
early Pliocene	26X-2, 19–21		No glass	No
	113-696B-			
early Pliocene	3R-4, 143–145		No glass	No
early Pliocene	5R-6, 135–137	15	1	Yes
early Pliocene	49R-1, 65–67		No glass	No
	113-697A-			
early Pliocene	1H-2, 52–54		No glass	No
	113-697B-			
early Pliocene	14X-1, 40–42		No glass	No
early Pliocene	14X-1, 80–82		No glass	No
early Pliocene	14X-1, 110–112		No glass	No
early Pliocene	15X-2, 74–75		No glass	No
early Pliocene	32X-2, 73–75	19	3	Yes
early Pliocene	32X-2, 146–148	20	Disseminated	Yes

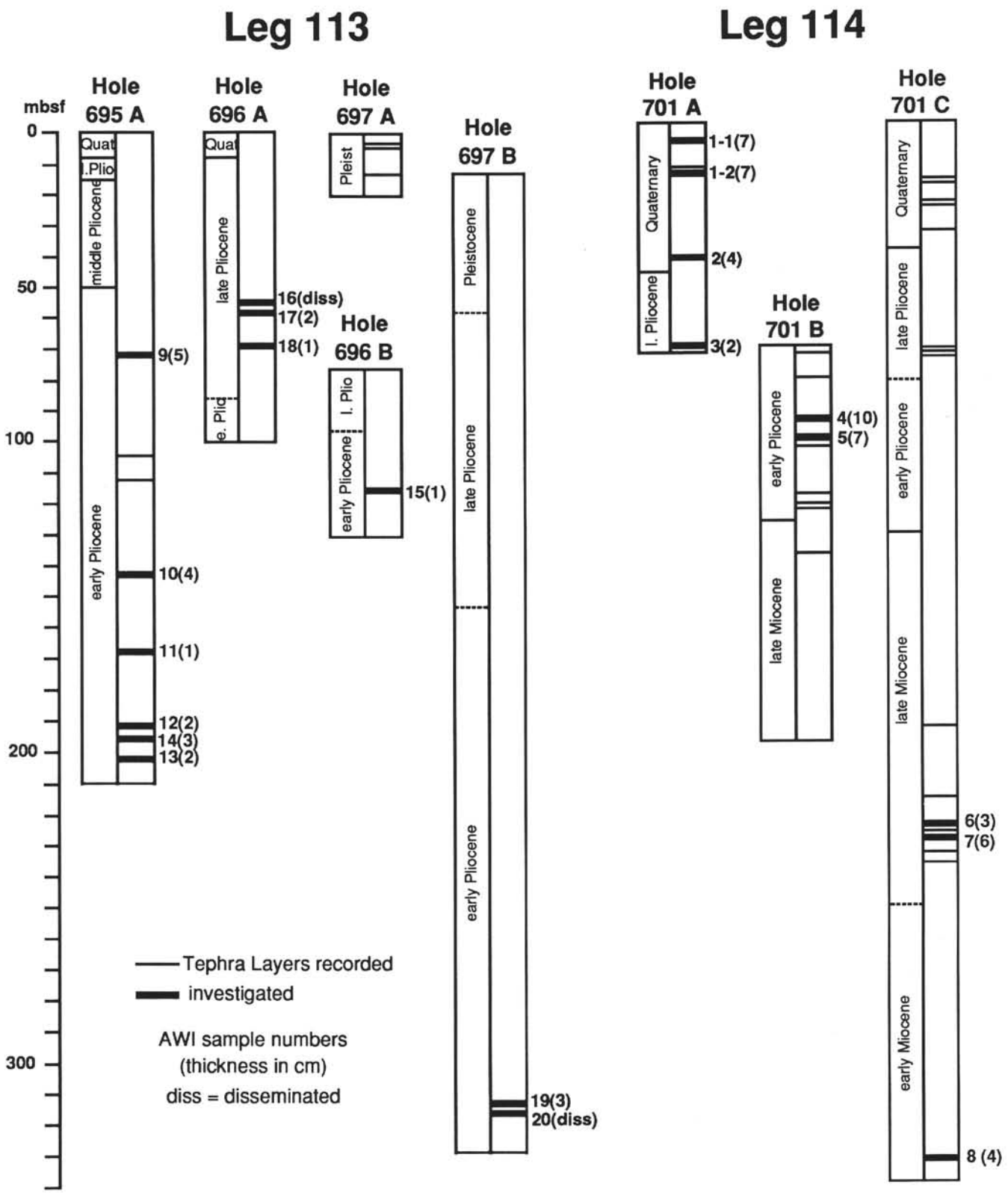

Figure 2. Schematic stratigraphy of the cored sections investigated in Holes 695A, 696A, 697A, and 697B (Barker, Kennett, et al., 1988) and 701A–701C (Ciesielski, Kristoffersen, et al., 1988).

Table 2. Analytical results obtained by EDX at Freiburg University with Smithsonian Institution reference glass and mineral standards.

Reference sample[a]	Analysis[b]	SiO_2	TiO_2	Al_2O_3	Cr_2O_3	FeO	MnO	MgO	CaO	K_2O	Na_2O
Glass	Smithsonian (mean)	51.11	1.86	14.14	0	11.91	0.22	6.75	11.18	0.19	2.64
111240	Freiburg (mean)	50.70	1.87	14.18	0	12.22	0.30	6.46	11.30	0.20	2.63
	(SD)	0.42	0.07	0.20	0	0.07	0.07	0.08	0.1	0.07	0.21
Glass	Smithsonian (mean)	77.19	0.12	12.14	0	1.24	0.03	0.09	0.50	4.92	3.77
72854	Freiburg (mean)	77.24	0	12.31	0	1.07	0	0	0.43	5.04	3.93
	(SD)	0.17	0	0.10	0	0.07	0	0	0.04	0.09	0.06
Plagioclase	Smithsonian (mean)	51.21	0.05	30.89	0	0.46	0	0.14	13.63	0.18	3.45
115900	Freiburg (mean)	52.11	0	30.30	0	0.40	0.04	0	13.48	0.09	3.58
	(SD)	0.26	0	0.06	0	0.03	0.08	0	0.17	0.06	0.15
Diopside	Smithsonian (mean)	55.13	0	0.11	0	0.24	0.04	18.39	25.75	0	0.34
117733	Frieburg (mean)	55.46	0	0.09	0	0.19	0	18.12	26.14	0	0
	(SD)	0.07	0	0.19	0	0.13	0	0.28	0.28	0	0
Cr-Augite	Smithsonian (mean)	50.41	0.51	8.02	0.85	4.68	0.12	17.30	17.28	0	0.84
164905	Frieburg (mean)	50.83	0.40	7.92	0.82	4.56	0	17.72	17.05	0	0.72
	(SD)	0.23	0.06	0.07	0.09	0.14	0	0.16	0.1	0	0.16
Hypersthene	Smithsonian (mean)	53.96	0.16	1.23	0.75	15.18	0.49	26.72	1.52	0	0
746	Frieburg (mean)	53.82	0.03	0.97	0.60	15.06	0.56	27.67	1.29	0	0
	(SD)	0.13	0.07	0.09	0.11	0.42	0.11	0.46	0.14	0	0
Hornblende	Smithsonian (mean)	40.88	4.78	15.09	0	11.06	0.09	12.96	10.43	2.08	2.63
143965	Freiburg (mean)	41.02	4.78	15.03	0	10.74	0.08	13.10	10.31	2.18	2.78
	(SD)	0.16	0.17	0.10	0	0.16	0.10	0.24	0.18	0.02	0.26

[a] Reference analysis number = USNM standard (Jarosewich et al., 1980).
[b] Freiburg mean and standard deviation are based on four analyses.

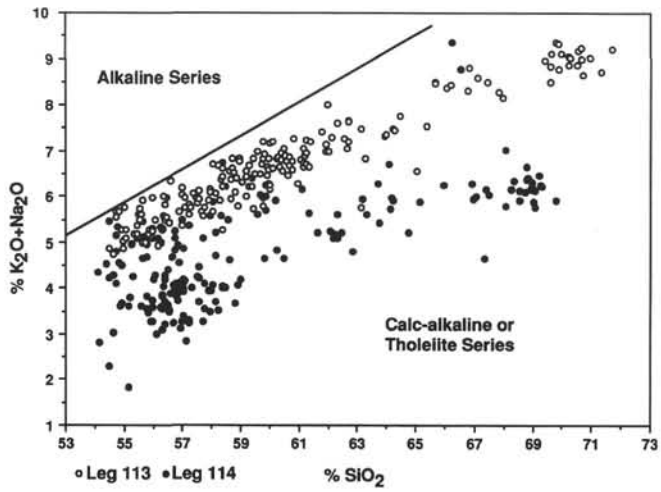

Figure 3. Total alkali-silica diagram of analyzed samples from Legs 113 and 114. The separation line of alkaline and calc-alkaline/tholeiitic rock series is according to MacDonald (1968).

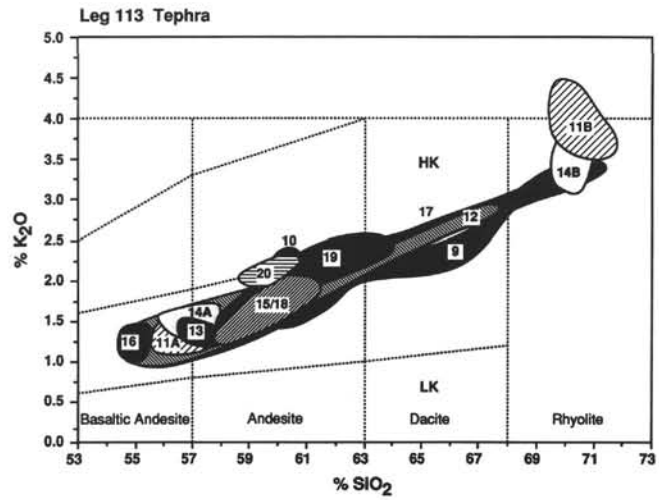

Figure 4. K_2O vs. SiO_2 of analyzed Leg 113 ashes. Individual ash layers are marked by their AWI sample numbers to show the range of variation for single layers (classification after Taylor et al., 1981). HK = high-potassium calc-alkaline rocks; LK = low-potassium calc-alkaline rocks.

ing time 100 s). Matrix correction was calculated according to a modified routine of Ware (1981). For calibration, standards from the Smithsonian Institution (Jarosewich et al., 1980) were used. Selected analyses are given in Table 2.

RESULTS

All the tephra layers investigated are of calc-alkaline composition ranging from island-arc tholeiites to high-potassium calc-alkaline series (Figs. 3–5).

Petrography

A summary of the important petrographic features of the ash layers is given in Table 3. Most of the glass shards investigated are very dark to pale brown in color, although some samples consist of at least two populations of colorless and brown glass. Glass textures range from dense, poorly vesicular blocky shards to highly vesicular particles with a pumiceous or elongated, fibrous habit. Some extremely vesicular types exhibit a bubble-wall texture (platy, cuspate shards). Fusiform (melt) structures were also found, indicating an overheated, low-viscosity magma during the eruption phase. Plates 1 and 2 show the structures most commonly observed. Some of the tephra layers contain glass shards shattered by numerous cracks (see Table 3), which are interpreted as the effect of shock cooling of the magma on contact with water or ice. The blocky to cuspate shards suggest phreatomagmatic to Plinian styles of eruption (cf. Heiken and Wohletz, 1985), in the latter case admitting the possibility of distant source areas for the ash layers. Tiny mineral inclusions, such as Fe-Ti oxides and pyroxenes, are commonly present, especially in the dark brown glasses.

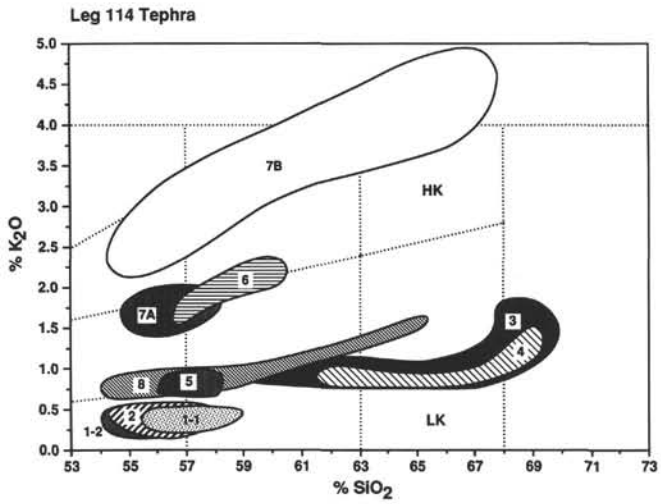

Figure 5. K_2O vs. SiO_2 of analyzed Leg 114 ashes. Individual ash layers are marked by their AWI sample numbers (classification after Taylor et al., 1981). HK = high-potassium calc-alkaline rocks; LK = low-potassium calc-alkaline rocks.

Leg 113

The mineral assemblages from Leg 113 are quite uniform, consisting of plagioclase, clinopyroxene, opaque minerals, and very rare orthopyroxene or pigeonite, all of which are thought to be phenocrysts. According to the microanalyses, An contents of the weakly zoned plagioclases are between An_{13} and An_{86}, reflecting a long range of fractionation from a similar parent magma composition for all the Leg 113 ash layers. The clinopyroxenes can be characterized as diopsidic augites and augites. No olivine was detected in either the Leg 113 or the Leg 114 tephras, despite their partially basic geochemistry.

Additional accessory minerals such as quartz, orthoclase, zircon, sphene, garnet, and amphibole are interpreted either as xenocrysts (originating from the wall rock during eruption) or, more likely, as terrigenous detritus derived from the southern slopes of the South Orkney Microcontinent.

Leg 114

Despite their overall similar mineralogy (plagioclase, clinopyroxene, opaque minerals, ± pigeonite and/or orthopyroxene; Table 3), three groups of tephras can be distinguished in the Leg 114 samples on the basis of their mineral assemblages. The four youngest ash layers (samples AWI1-1, AWI1-2, AWI2, and AWI3; late Pliocene–Quaternary) are characterized by the common occurrence of pigeonite, ± orthopyroxene, and relatively An-rich plagioclases (An_{45-85}). In contrast, two of the lower Miocene layers (samples AWI6 and AWI7) contain no orthopyroxenes and clearly have lower An contents in the plagioclases (An_{25-83}), as well as additional sanidine as a minor constituent, indicating a more highly evolved (high-potassium) calc-alkaline rock series. The mineralogy of the remaining ash layers varies between these two extremes (Table 3).

The very low abundance of detrital minerals at Site 701, as well as the different mineralogy of this fraction (quartz, garnet, and orthoclase), contrasts with that of the samples from Leg 113 and reflects the intraoceanic position of this site, far from terrigenous influence.

Geochemistry

Table 4 presents the mean values of chemical data from about 400 analyses of individual glass shards from 12 Leg 113 samples and nine Leg 114 samples. The complete data set is listed in the Appendix.

The geochemistry of the ash layers shows a large variation in most of the major elements, both within and between the different layers. As shown in the plots of total alkalis or potassium against silica (Figs. 3–5) all the ashes investigated belong to the island arc series characterized by subduction-related calc-alkaline magma compositions and follow the classical fractionation trend. This trend, caused by a clinopyroxene/plagioclase/magnetite fractionation, is also seen in the other major elements; magnesium, iron, calcium, and titanium decrease with increasing silica contents, whereas sodium and potassium increase, as does the potassium/sodium ratio. Because potassium as a representative of the incompatible elements is the most useful parameter to discriminate between the ash layers investigated, we will focus on the potassium/silica relationship in the following discussion.

Leg 113

The ash samples from Leg 113 (Fig. 4) are all of Pliocene age and plot in a narrow field that classifies them as typical of a calc-alkaline series (using the potassium/silica classification scheme of Taylor et al., 1981). According to this classification, they range from basaltic andesite to rhyodacite in composition. Individual samples exhibit some variability within this field. Samples AWI9, AWI12, and AWI17 show a chemical variance that covers almost the entire field of the Leg 113 ashes. The ashes in samples AWI11 and AWI14 are distinctly bimodal in their composition, with one group of glass shards plotting at the basaltic andesite end of the field whereas the other population corresponds to a rather highly evolved rhyodacitic type. The remaining ashes have basic or intermediate compositions and are less variable. Ashes from samples AWI10, AWI19, and AWI20 fall within a field of somewhat higher potassium contents, with silica contents between 57% and 65%.

Leg 114

In contrast, the ash samples from Leg 114 have distinctly different geochemical patterns. Although similar in silica content to the Leg 113 samples, they display a broad range of potassium contents (Fig. 5). Three different fields can be observed, from which the ash layers of Site 701 are classified as island-arc tholeiitic, calc-alkaline, and high-potassium calc-alkaline series (according to Taylor et al., 1981). These correspond to three age groups, Quaternary, Pliocene, and Miocene, respectively, with the exception of the lower Miocene tephra layer (AWI8), which has a typical calc-alkaline composition. The youngest (Quaternary) ash layers of Hole 701A in samples AWI1-1, AWI1-2, and AWI2 show a very narrow range in composition and are represented by the island-arc tholeiitic field. The upper Pliocene ash layer (sample AWI3) in Hole 701A shows higher potassium contents and plots in a field within the calc-alkaline series. The two lower Pliocene ash layers from Hole 701B (samples AWI4 and AWI5) fall in the same field as ash layer sample AWI3. One of the two upper Miocene ash layers from Hole 701C (sample AWI7) displays a bimodal distribution, with one population of ashes belonging to the high-potassium calc-alkaline series (AWI7B) and the other population (AWI7A) plotting together with ash layer sample AWI6 in a rather narrow calc-alkaline field with intermediate potassium content. The oldest ash layer encountered from Legs 113 and 114, sample AWI8 of early Miocene age, shows a continuous calc-alkaline trend with silica contents from 54% to 68%.

Table 3. Petrographic summary of ashes studied from Legs 113 and 114.

Sample (interval in cm) and size fraction (μm)	Thickness (cm)	Crystals[a]	Glass	Morphology[b]	Color[c]
113-					
AWI9: 695A-9H2, 5–7	5	++	++	hv; +incl	br
63–125		+lith		blocky	pbr
				fibr,	cl
				bubble-rich,	
				tub	
AWI10: 695A-18X-4, 120–121	4	++	++	v; +incl	dbr
63–125				"cracked"	pbr
				blocky	
AWI11: 695A-21X-2, 68–70	1	+	+++	lv+incl to hv	dbr
63–125				fibr to bw	pbr to cl
				platy	
AWI12: 695A-23X-5, 61–63	2	++	++	hv;+bubbles	dbr
63–125				fibr, tub	pbr, cl
AWI13: 695A-25X-6, 3–5	2	+	++	v;	dbr
63–125				cracked	pbr
				blocky	
AWI14: 695A-25X-1, 89–91	3	+	++	lv to hv;	dbr
63–125				blocky	pbr to cl
AWI15: 696B-5R-6, 135–137	1	+	++	lv; blocky	(br)
63–125				fibr, +bubbles	lbr
				cracked	
AWI16: 696A-7H-3, 5–7	Disseminated	++	++	hv;	br
63–125		+lith		pum, fusi	pbr
AWI17: 696-7H-7, 53–55	2	++	++	v to hv;	dbr
63–125		+lith		block fibr,	pbr
				pum	
ANI18: 696A-9H-2, 4–6	1	++	++	hv; +incl	br
63–125		+lith		(blocky)	pbr
				fibr, +bubbles	
				pum, bw	
AWI19: 697B-32X-2, 73–75	3	+++	++	hv; blocky	(br)
63–125				cracked	pbr
				fibr	cl
AWI20: 697B-32X-2, 146–148	Disseminated	+++	++	hv; blocky	br
63–125				cracked	pbr
				pum, fibr	cl
114-					
AWI1-1: 701A-1H-4, 58–60	7	+	++	hv; +incl	(br)
total sample				pum	pbr
AWI1-2: 701A-2H-4, 17–18	7	+	++	hv; pum	(dbr)
total sample				fibr	pbr
				bubble-rich	
AWI2: 701A-5H-5, 58–59	4	+	++	v; +incl	black
63–125		+lith		blocky	grbr pbr
AWI3: 701A-8H-4, 55–56	2	+	++	lv; blocky	rbr
63–125				hv; fibr	pbr-cl
AWI4: 701B-3H-4, 84–86	10	+	++	hv;	rbr
63–125				fibr, fusi bw	pbr
AWI5: 701B-4H-1, 132–134	7	++	++	v; +incl	dgr
63–125				blocky	br
				(fibr)	pbr
AWI6: 701C-24H-7, 13–15	3	+	+++	v;	(br)
63–125				blocky	pbr
				palag (fibr)	
AWI7: 701C-25X-1, 143–145	6	++	++	lv;	grbr
63–125				blocky	pbr
				palag	
AWI8: 701C-37X-1, 126–128	4	+	++	v; +incl	br
63–125				blocky	(pbr)

DISCUSSION

The chemical compositions of the ash samples from Sites 695, 696, and 697 close to the South Orkney Microcontinent are typically calc-alkaline, ranging from basalt-andesitic through dacitic to rhyolitic in composition (Table 4 and Figs. 3 and 4). The small amount of variation in the potassium/silica plot (Fig. 4) makes distinction between individual samples from the whole group of Leg 113 ashes difficult. This argues for magma sources that resemble each other, in which magma generation occurred under comparable conditions (i.e., at rather similar depths and with similar degrees of partial melting in the mantle), although not necessarily erupted from the same volcanic area. The geochemistry is typical for magma generation in connection with a subduction zone. Within the magma chambers, various degrees of fractional crystallization led either to continuous compositions of the eruption products (zoned magma chambers), as observed in samples AWI9, AWI17, and AWI19, or to smaller chemical variabilities, as in samples AWI10, AWI12, AWI13, AWI15, AWI16, AWI18, and AWI20. Two distinctly different magmatic compositions must have coexisted at the same time for the formation of the two bimodal ash layers in samples AWI11 and AWI14. This can be explained by a compositionally zoned magma chamber with sharp boundaries or by eruptions triggered by magma mixing.

Table 3 (continued).

Clino-pyroxene[d]	Pigeonite	Ortho-pyroxene	Opaque minerals	Accessories	Plagioclase An content	Alkali feldspar	>200 μm
+	+	–	+	–	+ 53–59	Orthoclase +glass incl	+
+	–	+	+	Sphene Garnet Amphibole	++ 13–57	Orthoclase (Albite) (Sanidine)	–
+	–	–	+	Garnet	+ 21–86	Orthoclase Albite?	++
+	–	–	+++ (Ilm)	Zircon	++ 13–60	Orthoclase Albite?	+
+	–	–	+	Garnet Amphibole Glauconite	+ 57–71	–	+
+	–	–	+	Amphibole	+ 54–70	–	+
+ 2	–	+	+	Garnet	+ 56–69	Orthoclase Albite?	+
+	–	–	++	Garnet Not determined	+	Orthoclase	+
+	–	+	+	Garnet Amphibole	++ 28–79	Orthoclase Sanidine	+
+	–	–	+ (Ti-Mt) (Ilm)	Garnet Zircon Amphibole	+ 42–68	Orthoclase Sanidine Albite?	+
++ 2	–	–	+	Garnet Sphene Amphibole	+ Not determined	–	++
++ 2	–	+	+	Garnet Amphibole (bl-gr)	+ Not determined	–	+
+	+	–	+	–	++ 65–69	–	++
+	+	+	+	–	++ 64–73	–	++
+	+	+	+	Garnet	++ 45–88	Sanidine Albite?	–
+	+ (incl)	+	+ (Ti-Mt)	–	++ 58–81	–	–
+	–	–	+	Biotite	+ Not determined	–	–
+	+	–	+	Garnet	++ 65–75	Orthoclase	+
+	–	–	+	–	++ 25–82	Orthoclase	–
+	+	–	+ (Ti-Mt)	–	++ 30–83	Sanidine	+
+	–	–	+ (Ilm)	–	+ 54–55	Sanidine Albite?	–

Note: Mineralogy and An content determined by EDX analysis. ( ) = minor. Relative abundance of glass and mineral phases: – = not found; + = present; ++ = abundant; +++ = highly abundant.

[a] +lith = rich in lithic material.

[b] lv = low vesicularity; v = vesicular; hv = high vesicularity; +incl = rich in inclusions; palag = palagonitized; pum = pumiceous; fibr = fibrous; tub = tubular; fusi = fusiform; bw = bubble wall; "cracked" = shattered by polygonal cracks.

[c] dbr = dark brown; rbr = red brown; grbr = gray brown; br = brown; lbr = light brown; pbr = pale brown; cl = colorless.

[d] 2 = two different clinopyroxenes.

In determining possible sources for the ashes, it should be taken into account that the analyses were performed on the glass fractions of the samples, without considering the phenocryst content of the bulk sample. Variable amounts of mostly plagioclase, pyroxene, and opaque phenocrysts have been observed in most samples (Table 3). In consequence, the glass compositions presented here should be slightly more evolved than the bulk-rock analyses taken from the literature for comparison.

Comparisons of the potassium/silica data from the Leg 113 ashes with published analyses for the Antarctic Peninsula and the South Shetland Islands over the time interval concerned (Fig. 6; data from Saunders et al., 1980; Smellie et al., 1984)

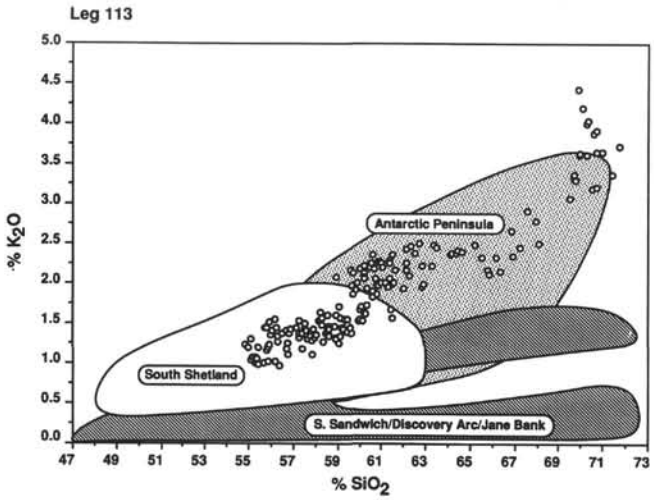

Figure 6. K_2O vs. SiO_2 of the Leg 113 analyses. The shaded fields indicate the composition of magmatic products from the South Shetland Islands (data from Smellie et al., 1984; Weaver et al., 1982), the Antarctic Peninsula (data from Saunders et al., 1980), and the South Sandwich Islands, Discovery Arc, and Jane Bank (data from Barker et al., 1984; Barker and Griffiths, 1972; Tomblin, 1979). Only those rocks that were formed during the same time period as the Leg 113 ashes are plotted.

show that there is only a weak correlation between the Leg 113 samples and the South Shetland Island analyses, but a much better correlation exists with those from the Antarctic Peninsula. It is not possible, however, to correlate individual ash layers with specific eruption sequences from the peninsula because of the sparse information on volcanism in this province.

Our data indicate that in a few cases compositional and stratigraphic correlation between holes is possible (e.g., the early Pliocene age layer AWI10 from Hole 695A and layers AWI19/AWI20 from Hole 697B). Furthermore, the layers in samples AWI12 and AWI13 (Hole 695A) correspond compositionally with layer AWI15 (Hole 696B).

The chemical analyses show that the Leg 114 samples are very different from those from Leg 113. Three different fractionation trends can be observed in the time span of the four stratigraphically defined groups (Fig. 5 and Table 1):

1. The Quaternary ash layers from Hole 701A (AWI1-1, AWI1-2, and AWI2) plot in the island-arc tholeiitic field with potassium contents of less than 0.5% (K_2O).
2. The Pliocene tephras from Holes 701A (AWI3) and 701B (AWI4 and AWI5) are typically calc-alkaline and are connected by a similar fractionation trend.
3. The upper Miocene ash layers from Hole 701C (AWI6 and AWI7) represent a unique high-potassium calc-alkaline fractionation trend.
4. The lower Miocene age tephra from Hole 701C (AWI8) also shows the typical calc-alkaline composition similar to the Pliocene ash layers.

It is obvious from these data that the various ash layers studied from Leg 114 cannot have formed from a common source of magma. The potassium-enriched calc-alkaline geochemistry of the Miocene ashes is believed to be typical of magma formation associated with subduction. The fact that potassium contents in the ashes of late Miocene age are higher than those of the early Miocene implies, however, different conditions of generation, possibly caused by a change in the inclination angle of the subducting plate. The composition of the late Miocene ash layer in sample AWI7 has a bimodal distribution that is believed to result from a change in magma compositions rather than from mixing of ashes from different eruptions. This sample was taken from a discrete ash layer, and it would have been rather fortuitous to have two volcanoes erupting at the same time from different locations.

The Pliocene ash layers from Holes 701A and 701B (AWI3, AWI4, and AWI5) plot within a common calc-alkaline field and were probably formed during the same mobilization process. Chemical compositions for the youngest ash layers (AWI1-1, AWI1-2, and AWI2) are different, indicating either a different geographic origin or a change in the magma-generation process.

Correlation of the Leg 114 ashes is somewhat difficult because there are only a few published geochemical analyses of the possible source areas. However, comparison with the available data (Fig. 7) shows that there is, in fact, a good correlation of the Quaternary ashes with analyses from the South Sandwich Islands, which form an island arc less than 4 (8?) Ma old (Baker, 1978; Barker and Griffiths, 1972; Tarney et al., 1982; Tomblin, 1979). The older calc-alkaline ashes (Pliocene samples AWI3, AWI4, and AWI5 and early Miocene sample AWI8) plot in the same field as the South Shetland Island volcanics, for which two cycles of activity in the Miocene and Pliocene have been reported (Smellie, 1983; Weaver et al., 1982). Our data provide supporting evidence of this.

No such correlation for the other Leg 114 ash layers (late Miocene age high-potassium calc-alkaline tephras) is possible at present, and determination of source areas must, therefore, await further detailed investigations. On the other hand, stratigraphic correlations suggest that the Pliocene and Miocene tephra layers may be derived from the now-extinct structures of the Discovery Arc and Jane Bank, respectively (Barker et al., 1982, 1984), taking into account the thickness of the layers (3–10 cm!). These structures are regarded as precursors of the South Sandwich Island Arc, now separated by the Southern Scotia Ridge transform fault. Unfortunately there are no representative reference samples from these arcs to test this hypothesis. Nev-

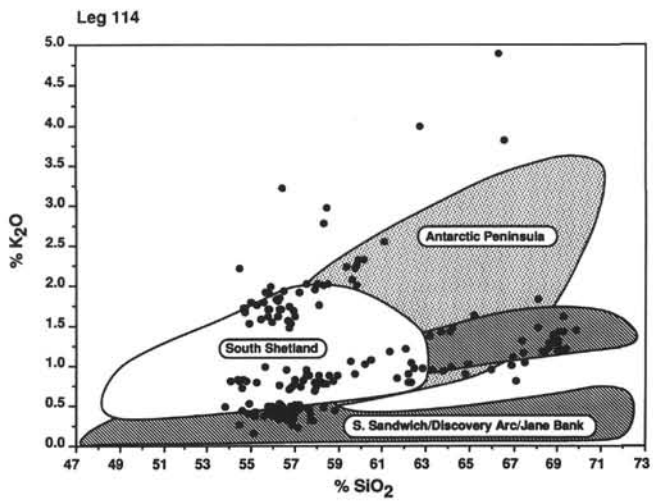

Figure 7. K_2O vs. SiO_2 of the Leg 114 analyses. The shaded fields indicate the composition of magmatic products from the South Sandwich Islands, Discovery Arc, and Jane Bank (data from Barker et al., 1984; Barker and Griffiths, 1972; Tomblin, 1979), the South Shetland Islands (data from Smellie et al., 1984; Weaver et al., 1982), and the Antarctic Peninsula (data from Saunders et al., 1980).

Table 4. Mean values of the chemical data from the ash layers studied from Legs 113 and 114.

Sample[a]		SiO_2 (%)	TiO_2 (%)	Al_2O_3 (%)	FeO (%)	MnO (%)	MgO (%)	CaO (%)	K_2O (%)	Na_2O (%)
AWI1-1	Mean	56.64	1.09	15.56	11.17	0.25	3.41	8.27	0.36	3.20
$N = 15$	SD	0.79	0.10	0.41	0.62	0.09	0.43	0.25	0.06	0.32
AWI1-2	Mean	56.21	1.14	15.04	11.69	0.30	3.67	8.46	0.39	2.99
$N = 21$	SD	0.84	0.08	0.71	0.66	0.25	0.73	0.61	0.09	0.46
AWI2	Mean	56.67	1.12	15.36	11.64	0.27	3.13	7.90	0.41	3.45
$N = 20$	SD	0.97	0.08	1.05	0.90	0.12	0.84	0.58	0.06	0.42
AWI3	Mean	67.48	0.77	14.77	6.06	0.11	0.28	4.44	1.18	4.83
$N = 21$	SD	1.79	0.13	0.87	0.86	0.10	0.38	0.60	0.21	0.43
AWI4A	Mean	61.52	1.02	15.09	9.38	0.23	1.76	6.18	0.82	3.92
$N = 5$	SD	3.33	0.09	0.20	1.31	0.06	1.26	1.52	0.20	0.66
AWI4B	Mean	69.00	0.66	13.97	6.22	0.03	0.04	3.83	1.29	4.82
$N = 9$	SD	0.18	0.08	0.17	0.15	0.07	0.10	0.18	0.10	0.28
AWI5	Mean	57.57	1.32	15.49	11.32	0.26	2.44	7.51	0.76	3.22
$N = 19$	SD	0.93	0.10	0.61	0.88	0.10	0.46	0.23	0.08	0.26
AWI6	Mean	58.39	1.23	15.81	10.0o4	0.24	1.93	6.49	1.99	3.75
$N = 17$	SD	1.32	0.08	0.39	0.59	0.08	0.48	0.56	0.22	0.18
AWI7A	Mean	55.86	1.11	16.23	10.38	0.20	3.08	8.03	1.75	3.29
$N = 29$	SD	0.82	0.13	0.58	0.72	0.11	0.42	0.40	0.34	0.26
AWI7B	Mean	62.23	1.18	15.79	7.53	0.08	1.07	4.53	3.50	3.99
$N = 6$	SD	3.62	0.14	0.71	2.63	0.13	1.00	0.86	0.90	0.63
AWI8	Mean	59.09	1.46	15.87	9.16	0.27	2.27	6.66	1.06	4.08
$N = 22$	SD	4.11	0.20	0.45	1.82	0.05	1.06	1.51	0.30	0.57
AWI9	Mean	63.63	1.04	16.28	6.14	0.07	0.85	4.17	2.12	5.58
$N = 23$	SD	3.98	0.39	0.86	1.53	0.11	0.97	1.61	0.63	0.52
AWI10	Mean	60.13	1.40	16.21	8.08	0.15	1.63	5.54	2.07	4.71
$N = 19$	SD	0.51	0.10	0.40	0.44	0.10	0.28	0.20	0.20	0.36
AWI11A	Mean	56.35	1.45	16.99	9.28	0.19	2.79	7.42	1.36	4.14
$N = 13$	SD	0.92	0.15	0.46	0.72	0.10	0.37	0.30	0.11	0.34
AWI11B	Mean	70.42	0.33	14.55	3.75	0.08	0.00	1.57	3.89	5.21
$N = 11$	SD	0.57	0.11	0.13	0.33	0.12	0.00	0.17	0.27	0.26
AWI12A	Mean	56.65	1.50	16.62	9.34	0.18	2.74	7.14	1.31	4.49
$N = 13$	SD	1.58	0.17	0.29	0.83	0.11	0.41	0.59	0.21	0.40
AWI12B	Mean	64.50	0.92	16.27	5.94	0.07	0.73	4.32	2.40	4.67
$N = 5$	SD	2.20	0.23	0.61	1.81	0.10	0.52	0.85	0.27	0.84
AWI13	Mean	57.45	1.44	16.56	9.01	0.22	2.54	6.77	1.38	4.53
$N = 8$	SD	0.68	0.09	0.47	0.57	0.10	0.30	0.24	0.06	0.26
AWI14A	Mean	64.51	0.86	15.27	6.43	0.11	1.14	4.06	2.51	4.99
$N = 6$	SD	1.00	0.06	0.36	0.79	0.12	0.34	0.27	0.11	0.35
AWI14B	Mean	70.27	0.35	14.47	4.01	0.09	0.00	1.73	3.34	5.58
$N = 8$	SD	0.41	0.03	0.07	0.10	0.10	0.00	0.09	0.19	0.17
AWI15	Mean	59.48	1.16	16.06	8.74	0.22	2.11	5.85	1.65	4.64
$N = 10$	SD	1.24	0.07	0.42	0.51	0.09	0.36	0.59	0.22	0.46
AWI16	Mean	55.09	1.44	16.54	10.12	0.15	3.46	8.05	1.11	4.03
$N = 12$	SD	0.49	0.08	0.16	0.29	0.12	0.16	0.20	0.12	0.34
AWI17	Mean	60.17	1.12	16.20	7.82	0.16	2.09	5.74	1.71	4.94
$N = 18$	SD	4.65	0.34	0.67	1.69	0.09	1.45	2.15	0.64	0.64
AWI18	Mean	59.54	1.37	16.17	8.43	0.20	1.82	5.84	1.57	5.01
$N = 12$	SD	1.41	0.23	0.50	1.20	0.11	0.54	0.45	0.28	0.36
AWI19	Mean	61.36	1.07	15.93	7.59	0.24	1.54	5.39	2.04	4.68
$N = 17$	SD	2.09	0.12	0.58	0.75	0.08	0.53	0.87	0.32	0.34
AWI20	Mean	60.91	1.26	15.90	7.93	0.19	1.51	5.31	2.28	4.56
$N = 11$	SD	1.08	0.12	0.22	0.60	0.10	0.27	0.51	0.15	0.27

[a] Two different populations in an ash layer are labeled *A* and *B*. N = number of glass shards analyzed from a single ash layer.

ertheless, the tephra samples studied plot in the field of the published analyses (Fig. 7).

Ciesielski, Kristoffersen, et al. (1988) suggested eruptions in the southern Andes also as potential sources for the tephra layers. Correlation of such thick and distinct airborne(?) tephra layers with eruptions from the calc-alkaline volcanic centers of South America seems rather unlikely because of the large distances involved (approximately 3500 km). Only minor or trace amounts of disseminated volcanic ash of Oligocene to Holocene age are reported from the Falkland Plateau area, which is in an even closer position with respect to South America (Deep Sea Drilling Project Leg 36; Elliot and Emerick, 1977). Of course, additional distribution of tephra by ice rafting has to be considered, but cannot be evaluated here.

CONCLUSIONS

The volcanic ash samples studied from ODP Legs 113 and 114 in the southern Atlantic–Antarctic cover the whole field of the calc-alkaline suite, ranging from basaltic andesites to andesites, dacites, and rhyolites, and are classified as island-arc tholeiitic, calc-alkaline, and high-potassium calc-alkaline rock series on the basis of their potassium/silica ratios.

On a stratigraphic basis three age groups are recognized:

1. Quaternary ashes (Leg 114);
2. Pliocene ashes (Legs 113 and 114);
3. Miocene ashes (Leg 114).

Ash samples from Leg 113 Sites 695, 696, and 697, close to the South Orkney Microcontinent, are Pliocene in age and belong to a normal calc-alkaline suite ranging from basaltic andesites to dacites and rhyolites. Their restriction to a very narrow field of evolution argues for a common subduction-related origin. The source volcanoes for these ashes are believed to be on the Antarctic Peninsula.

The variable potassium contents of the ashes from Site 701 of Leg 114 allow them to be grouped in three separate magmatic series. The oldest investigated tephra, of early Miocene age, has a calc-alkaline composition and could be derived from the Miocene activity of the South Shetland Island Arc. Late Miocene tephra layers have the highest potassium contents and plot in the high-potassium calc-alkaline field. The Miocene tephras could alternatively stem from the now-extinct Discovery Arc or Jane Bank, the ancestors of the South Sandwich Islands Arc. It is not possible at the present stage of investigation to determine a distinct source region for these ashes, because of the lack of representative reference samples. The Pliocene ashes can be separated into different geochemical fields indicating different origins. Early and late Pliocene age ashes having a classic calc-alkaline composition probably originate from the South Shetland Islands. The Quaternary samples, displaying low potassium contents that classify them as island-arc tholeiites, are most likely derived from the South Sandwich Islands.

ACKNOWLEDGMENTS

We wish to thank Heike Ostermann (Alfred-Wegener-Institute) and Erika Lutz (Freiburg University) for technical help and assistance during sample processing and microprobe measurements. We are grateful to Dr. W. Ehrmann (AWI) for critically reviewing this manuscript, and we address our compliments to two reviewers and to P. Ciesielski for the editorial handling. Financial support by the Deutsche Forschungsgemeinschaft (Grant Fu 119/14) is acknowledged. This is AWI publication no. 187.

REFERENCES

Baker, P. E., 1978. *The South Sandwich Islands: III. Petrology of the Volcanic Rocks*: Sci. Rept. Br. Antarct. Surv., 93.

Barker, P. F., Barber, P. L., and King, E. C., 1984. An early Miocene ridge-crest collision on the South Scotia Ridge near 36°W. *Tectonophysics*, 102:315–332.

Barker, P. F., and Griffiths, D. H., 1972. The evolution of the Scotia Ridge and Scotia Sea. *Philos. Trans. R. Soc. London, A*, 271:151–183.

Barker, P. F., Hill, A., Weaver, S., and Pankhurst, R., 1982. The origin of the eastern South Scotia Ridge as an intra-oceanic island-arc. *In* Craddock, C. (Ed.), *Antarctic Geoscience*: Madison (Univ. Wisconsin Press), 203–211.

Barker, P. F., Kennett, J. P., et al., 1988. *Proc. ODP, Init. Repts.*, 113: College Station, TX (Ocean Drilling Program).

Ciesielski, P., Kristoffersen, Y., et al., 1988. *Proc. ODP, Init. Repts.*, 114: College Station, TX (Ocean Drilling Program).

Dalziel, I.W.D., 1983. The evolution of the Scotia arc: a review. *In* Oliver, R. L., James, P. R., and Jago, J. B. (Eds.), *Antarctic Earth Science*: Canberra (Austral. Acad. Sci.), 283–288.

Elliot, D. H., and Emerick, C. M., 1976. Volcanic glass in some DSDP Leg 36 cores. *In* Barker, P. F., Dalziel, I.W.D., et al., *Init. Repts. DSDP*, 36: Washington (U.S. Govt. Printing Office), 871–876.

Federman, A. N., Watkins, N. D., and Sigurdsson, H., 1982. Scotia Arc volcanism recorded in abyssal piston cores downwind from the islands. *In* Craddock, C. (Ed.), *Antarctic Geoscience*: Madison (Univ. Wisconsin Press), 223–238.

Gonzalez-Ferran, O., 1982. The Antarctic Cenozoic tectonic processes. *In* Craddock, C. (Ed.), *Antarctic Geoscience*: Madison (Univ. Wisconsin Press), 687–694.

Heiken, G., and Wohletz, K., 1985. *Volcanic Ash*: Berkeley (Univ. of California Press).

Jarosewich, E., Nelen, J. A., and Norberg, J. A., 1980. Reference samples for electron microprobe analysis. *Geostandards Newslett.*, 4:43–47.

Keller, R. A., Fisk, M. R., White, W. M., and Birkenmajer, K., 1988. Late Tertiary-Quaternary transition from arc to back-arc volcanism, South Shetland Islands and Bransfield Strait, Antarctica. *EOS, Trans. Am. Geophys. Union*, 44:1471.

MacDonald, G. A., 1968. Composition and origin of Hawaiian lavas. *In* Coats, R. R., Hay, R. L., and Anderson, C. A. (Eds.), *Studies in Volcanology: A Memoir in Honor of Howel Williams*. Geol. Soc. Am. Mem., 116:477–522.

Morche, W., 1988. Tephrochronologie der Äolischen Inseln [Ph.D. dissert.]. Mineralogisch-Petrographisches Institut der Universität Freiburg/Br.

Ninkovich, D., Heezen, B. C., Conolly, J. R., and Burckle, L. H., 1964. South Sandwich tephra in deep-sea sediments. *Deep-Sea Res., Part A*, 11:605–619.

Saunders, A. D., Tarney, J., and Weaver, S. D., 1980. Transverse geochemical variations across the Antarctic Peninsula: implications for the genesis of calc-alkaline magmas. *Earth Planet. Sci. Lett.*, 46:344–360.

Smellie, J. L., 1983. A geochemical overview of subduction-related igneous activity in the South Shetland Islands, Lesser Antarctica. *In* Oliver, R. L., James, P. R., Jago, J. B. (Eds.), *Antarctic Earth Science*: Canberra (Austral. Acad. Sci.), 352–356.

Smellie, J. L., Pankhurst, R. J., Hole, M. J., and Thomson, J. W., 1988. Age, distribution and eruptive conditions of late Cenozoic alkaline volcanism in the Antarctic Peninsula and Eastern Ellsworth Land: a review. *Bull. Br. Antarct. Surv.*, 80:21–49.

Smellie, J. L., Pankhurst, R. J., Thomson, M.R.A., and Davies, R.E.S., 1984. *The Geology of the South Shetland Islands: VI. Stratigraphy, Geochemistry and Evolution*. Sci. Rept. Br. Antarct. Surv., 87.

Smith, D. G., Ledbetter, M. T., and Ciesielski, P. F., 1983. Ice-rafted volcanic ash in the South Atlantic sector of the Southern Ocean during the last 100,000 years. *Mar. Geol.*, 53:291–312

Tarney, J., Weaver, S. D., Saunders, A. D., Pankhurst, R. J., and Barker, P. F., 1982. Volcanic evolution of the northern Antarctic Peninsula and the Scotia Arc. *In* Thorpe, R. S. (Ed.), *Andesites: Orogenic Andesites and Related Rocks*: Chichester (Wiley), 371–400.

Taylor, S. R., Arculus, R., Perfit, M. R., and Johnson, R. W., 1981. Island arc basalts. *In Basaltic Volcanism on the Terrestrial Planets*: New York (Pergamon Press), 193–213.

Tomblin, J. F., 1979. *The South Sandwich Islands: II. The Geology of Candlemas Islands*. Sci. Rept. Br. Antarct. Surv., 92.

Ware, N. G., 1981. Computer programs and calibration with PIBS technique for quantitative electron probe analysis using a lithium-drifted silicon detector. *Comput. Geosci.*, 7:167–184.

Weaver, S. D., Saunders, A. D., Pankhurst, R. J., and Tarney, J., 1979. A geochemical study of magmatism associated with the initial stages of back-arc spreading: the Quaternary rocks of Bransfield Strait, South Shetland Islands. *Contrib. Mineral. Petrol.*, 68:151–169.

Weaver, S. D., Saunders, A. D., and Tarney, J., 1982. Mesozoic-Cenozoic volcanism in the South Shetland Islands and the Antarctic Peninsula: geochemical nature and plate-tectonic significance. *In* Craddock, C. (Ed.), *Antarctic Geoscience*: Madison (Univ. Wisconsin Press), 263–273.

Date of initial receipt: 24 March 1989
Date of acceptance: 27 October 1989
Ms 114B-182

APPENDIX

Chemical Elements of Analyzed Glass Samples, Legs 113 and 114

Data set is normalized to 100% water free. Original sums range approximately between 93% and 98%, depending on the volatile content and measured bubble-free surface.

Sample	SiO_2 (%)	TiO_2 (%)	Al_2O_3 (%)	FeO (%)	MnO (%)	MgO (%)	CaO (%)	K_2O (%)	Na_2O (%)
Leg 114									
AWI1-1	55.60	1.16	15.47	11.61	0.04	3.79	8.52	0.35	3.26
	55.79	1.08	15.38	11.64	0.30	3.64	8.52	0.38	3.18
	55.97	1.14	15.32	11.34	0.36	3.85	8.36	0.35	3.24
	56.13	1.15	15.49	12.02	0.27	3.41	8.52	0.38	2.63
	56.30	1.15	15.18	11.39	0.33	3.78	8.20	0.31	3.30
	56.37	1.29	16.24	11.04	0.18	2.27	8.49	0.50	3.55
	56.43	1.11	15.29	11.63	0.23	3.57	8.12	0.34	3.27
	56.47	1.00	15.38	11.57	0.18	3.47	8.31	0.37	3.25
	56.52	1.26	15.23	11.11	0.34	3.56	8.26	0.35	3.28
	56.55	1.09	15.30	11.32	0.26	3.64	8.32	0.34	3.18
	56.70	0.96	16.74	9.84	0.21	3.11	8.29	0.32	3.76
	56.91	0.96	15.42	11.56	0	3.69	8.25	0.37	2.74
	57.14	1.10	15.73	11.02	0.20	3.57	8.34	0.22	2.61
	57.77	0.91	15.74	10.72	0.38	2.74	8.11	0.39	3.16
	58.89	1.02	15.54	9.77	0.21	3.03	7.49	0.42	3.64
AWI1-2	54.48	1.02	13.48	12.50	0.23	6.26	9.70	0.24	2.06
	54.63	1.24	14.09	12.57	0.38	4.75	9.13	0.42	2.61
	55.16	1.08	13.97	12.64	0.23	4.54	10.55	0.15	1.68
	55.18	1.23	14.94	11.91	1.32	3.67	8.14	0.36	3.25
	55.22	1.21	15.31	11.59	0.34	3.91	8.48	0.40	3.39
	55.82	1.23	15.03	11.89	0.37	3.34	8.66	0.48	2.99
	55.96	1.14	15.34	11.49	0.30	3.65	8.32	0.38	3.35
	55.98	1.18	15.46	11.79	0.29	3.50	8.39	0.47	2.80
	56.27	1.27	15.11	11.86	0.22	3.21	8.38	0.45	3.14
	56.29	1.15	15.39	11.00	0.36	3.63	8.14	0.43	3.44
	56.32	1.34	13.10	13.65	0.26	3.98	8.12	0.52	2.56
	56.42	1.06	15.36	11.15	0.30	3.58	8.32	0.37	3.34
	56.53	1.08	15.32	11.51	0.25	3.48	8.21	0.35	3.15
	56.61	1.15	15.51	11.15	0.32	3.13	8.14	0.42	3.46
	56.67	1.04	15.53	11.55	0.30	3.35	8.32	0.32	2.93
	56.85	1.02	15.67	11.22	0	3.25	8.19	0.37	3.35
	56.97	1.10	15.51	11.19	0.19	3.46	8.31	0.31	2.96
	57.01	1.12	15.54	11.16	0	3.04	8.13	0.40	3.51
	57.22	1.16	15.61	10.96	0.20	3.25	8.29	0.45	2.79
	57.22	1.15	15.27	11.62	0.28	2.99	8.01	0.49	2.82
	57.56	1.03	15.33	11.14	0.22	3.19	7.82	0.46	3.25
AWI2	54.16	1.12	15.75	11.72	0.29	4.14	9.92	0.45	2.36
	54.88	1.23	13.92	12.79	0.33	4.93	8.24	0.38	3.23
	55.80	1.14	16.67	11.27	0.16	2.60	8.41	0.41	3.43
	56.03	1.12	15.29	11.82	0.42	3.55	7.53	0.40	3.78
	56.05	1.02	16.07	11.16	0.24	2.91	8.22	0.35	3.93
	56.30	1.21	13.77	12.57	0.41	4.63	7.55	0.39	3.17
	56.39	0.91	16.54	10.83	0.32	2.76	7.97	0.34	3.95
	56.42	1.12	13.32	13.27	0.24	4.04	8.27	0.47	2.73
	56.81	1.20	15.38	12.18	0	2.40	7.82	0.48	3.63
	56.85	1.12	14.91	12.25	0.38	3.16	7.37	0.44	3.45
	56.95	1.17	15.80	11.18	0.22	2.77	7.91	0.34	3.65
	56.95	1.14	15.29	11.69	0.35	2.75	7.61	0.44	3.70
	57.03	1.16	14.90	12.07	0.19	2.89	7.48	0.43	3.75
	57.04	1.15	15.35	11.92	0.42	3.08	7.63	0.39	3.02
	57.04	1.18	16.56	10.83	0.24	1.77	8.15	0.49	3.64
	57.07	1.18	14.84	12.08	0.36	3.06	7.25	0.45	3.71
	57.71	1.12	13.58	12.67	0.35	4.01	7.27	0.46	2.82
	57.90	0.94	16.39	10.41	0	2.81	7.49	0.30	3.66
	58.36	1.09	16.92	9.60	0.18	1.55	8.12	0.46	3.58
AWI3	59.01	1.53	14.47	12.15	0.20	2.33	5.48	0.89	3.95
	59.80	1.24	15.28	10.61	0.18	1.70	6.55	0.88	3.77
	62.17	0.87	16.47	7.61	0.28	1.44	6.10	0.78	4.29
	62.21	1.01	15.26	8.62	0.24	1.57	5.90	0.89	4.29
	62.29	0.97	15.37	8.34	0	1.86	5.97	0.77	4.32
	62.32	1.01	15.39	8.17	0.19	1.51	5.74	1.03	4.58
	63.32	0.88	15.56	7.74	0.21	1.08	5.55	0.93	4.68
	63.74	0.88	15.69	7.66	0	1.17	5.45	0.92	4.49
	64.12	0.99	15.07	7.58	0.18	0.96	5.39	0.97	4.75
	65.95	0.54	16.77	5.08	0.18	0	5.12	0.93	5.33
	66.89	0.68	16.10	5.32	0	0	4.72	0.99	5.29
	66.96	0.68	14.61	6.57	0	0.69	4.43	1.10	4.86
	67.06	0.68	15.91	5.27	0	0	5.00	0.79	5.22

Appendix (continued).

Sample	SiO_2 (%)	TiO_2 (%)	Al_2O_3 (%)	FeO (%)	MnO (%)	MgO (%)	CaO (%)	K_2O (%)	Na_2O (%)
	67.33	1.05	14.43	7.67	0	0	4.70	1.33	3.33
	67.39	0.80	14.59	6.04	0.26	0.56	4.14	1.15	5.02
	67.48	0.57	16.18	4.96	0	0	4.77	1.02	5.01
	68.07	0.92	13.94	6.01	0	0.33	4.74	1.47	4.32
	68.27	0.66	14.20	6.08	0.20	0.33	4.03	1.16	4.99
	68.35	0.69	14.18	5.96	0.17	0.29	3.96	1.17	5.16
	68.55	0.95	14.10	5.99	0	0	4.34	1.28	4.65
	68.56	0.76	14.16	5.92	0.17	0	4.32	1.22	4.90
	68.76	0.73	14.19	5.60	0.19	0.23	3.78	1.32	5.05
	68.76	0.74	13.99	5.61	0.21	0	3.93	1.31	5.33
	69.14	0.64	14.18	5.75	0.19	0.30	3.76	1.20	4.76
	69.22	0.84	14.11	5.41	0.23	0	3.52	1.60	4.87
	69.24	0.78	14.27	5.27	0	0	4.04	1.42	4.83
	69.81	0.76	13.87	5.70	0.16	0	3.65	1.43	4.50
AWI4A	55.93	1.04	15.35	11.33	0.22	3.98	8.88	0.48	2.79
	61.63	1.07	14.89	9.86	0.18	1.37	5.68	0.83	4.38
	62.46	1.02	15.12	8.72	0.32	1.48	5.58	0.96	4.24
	62.83	1.10	15.21	9.16	0.24	0.99	5.57	0.95	3.86
	64.76	0.87	14.89	7.85	0.18	1.00	5.17	0.89	4.31
AWI4B	68.74	0.68	13.74	6.37	0	0	4.17	1.38	4.71
	68.84	0.67	14.04	6.02	0	0.28	3.60	1.28	5.13
	68.93	0.64	14.09	6.30	0	0	3.78	1.28	4.87
	68.98	0.64	14.04	6.19	0	0	3.85	1.18	5.05
	68.98	0.61	15.60	4.43	0	0	3.92	1.31	5.00
	69.04	0.73	13.88	6.29	0	0	3.99	1.42	4.47
	69.09	0.60	14.21	6.11	0	0	3.69	1.18	4.95
	69.09	0.78	13.75	6.42	0.20	0	3.83	1.41	4.36
	69.32	0.50	14.03	6.03	0	0	3.76	1.21	5.02
AWI5	54.94	1.44	13.90	14.28	0.28	3.38	8.04	0.52	3.16
	56.29	1.40	15.05	12.17	0.31	3.05	7.78	0.75	3.08
	56.75	1.24	15.70	11.35	0.42	2.98	7.41	0.69	3.30
	56.89	1.41	16.01	10.72	0.37	2.47	7.51	0.73	3.83
	57.04	1.36	15.31	11.72	0.32	2.56	7.61	0.76	3.22
	57.04	1.40	15.58	11.05	0.29	2.68	7.68	0.81	3.30
	57.31	1.19	15.91	11.10	0.27	2.47	7.63	0.73	3.29
	57.49	1.27	15.45	11.12	0.29	2.51	7.51	0.75	3.50
	57.55	1.33	14.92	11.31	0.32	3.08	7.13	0.87	3.35
	57.58	1.60	14.82	12.14	0.34	1.62	7.25	0.94	3.54
	57.92	1.31	15.62	11.34	0.31	2.42	7.50	0.78	2.72
	57.97	1.23	16.11	10.66	0.28	2.37	7.38	0.67	3.27
	58.04	1.27	16.13	10.87	0	1.81	7.73	0.73	3.33
	58.11	1.30	15.54	11.16	0	2.49	7.63	0.77	2.93
	58.25	1.30	15.00	11.57	0.25	2.51	7.56	0.77	2.74
	58.37	1.34	16.90	9.62	0.26	1.80	7.60	0.76	3.25
	58.45	1.25	15.56	10.76	0.19	2.34	7.44	0.76	3.25
	58.80	1.16	15.59	11.12	0.20	2.07	7.28	0.79	2.87
	59.00	1.35	15.21	11.08	0.20	1.82	7.06	0.86	3.32
AWI6	56.31	1.25	16.18	10.84	0.21	2.48	7.38	1.69	3.58
	56.37	1.24	15.69	10.92	0.28	2.72	7.11	1.70	3.87
	56.72	1.25	16.23	10.77	0.22	2.39	7.17	1.56	3.68
	56.97	1.33	16.00	10.63	0	2.13	7.28	1.67	3.82
	57.23	1.26	15.28	10.65	0.29	2.79	6.99	1.91	3.44
	57.53	1.31	15.54	10.36	0.29	2.17	6.76	2.01	3.85
	57.96	1.13	16.10	9.98	0.29	2.03	6.75	1.94	3.65
	58.05	1.30	15.96	9.89	0.31	1.99	6.49	2.01	3.86
	58.34	1.34	15.65	10.03	0.35	2.02	6.46	1.99	3.58
	58.54	1.10	15.65	10.21	0.34	1.98	6.55	2.02	3.47
	59.36	1.20	15.67	9.57	0.20	1.64	5.85	2.22	4.18
	59.66	1.26	15.51	9.97	0.20	1.38	5.85	2.07	3.98
	59.75	1.16	15.42	9.85	0.17	1.57	5.99	2.21	3.76
	59.85	1.01	16.94	8.70	0.25	0.99	6.45	2.00	3.70
	59.85	1.19	15.80	9.53	0.17	1.50	5.85	2.25	3.77
	59.87	1.28	15.51	9.55	0.32	1.51	5.61	2.32	3.92
	60.18	1.24	15.57	9.27	0.26	1.60	5.78	2.31	3.61
	54.47	1.55	14.72	12.59	0	3.15	7.95	2.20	3.24
	54.71	1.29	15.93	10.90	0.18	3.46	8.26	1.71	3.44
	54.73	1.20	15.73	11.43	0.24	3.37	8.36	1.66	3.16
	54.76	1.15	16.53	10.84	0.28	3.06	7.95	1.72	3.62
	54.91	1.03	16.00	10.04	0.19	4.36	9.20	1.25	3.02
	54.92	1.13	17.01	10.30	0.19	3.10	8.72	1.52	2.98
	55.00	1.16	15.59	11.10	0.21	3.74	8.16	1.79	3.25
	55.27	1.17	15.82	10.68	0.26	3.42	8.30	1.75	3.22
	55.44	0.92	17.67	9.33	0.24	2.75	8.46	1.58	3.52
	55.62	1.25	16.60	10.12	0.19	2.97	7.73	1.78	3.67
	55.68	1.11	15.87	11.14	0	3.06	7.91	1.91	3.22
	55.77	0.99	16.34	10.05	0.27	3.40	8.42	1.61	3.09
	55.78	1.08	16.26	9.87	0.19	3.32	8.40	1.69	3.27

Appendix (continued).

Sample	SiO_2 (%)	TiO_2 (%)	Al_2O_3 (%)	FeO (%)	MnO (%)	MgO (%)	CaO (%)	K_2O (%)	Na_2O (%)
	55.80	0.90	16.83	9.41	0.22	3.65	8.69	1.22	3.28
	55.83	1.27	16.21	10.63	0.34	2.92	7.61	1.69	3.44
	55.86	1.05	16.31	10.23	0.31	2.87	8.10	1.89	3.32
	55.95	1.10	16.23	10.76	0.34	2.56	7.68	1.97	3.32
	55.99	0.97	16.77	9.76	0.32	3.17	7.92	1.54	3.56
	56.18	1.18	16.08	11.07	0	2.55	7.78	1.82	3.26
	56.24	1.03	16.25	10.01	0.25	3.28	7.56	1.60	3.72
	56.25	1.15	16.03	10.30	0.29	3.08	7.82	1.80	3.20
	56.33	1.16	16.11	9.97	0.29	3.06	7.69	1.83	3.48
	56.45	1.16	15.03	9.91	0.16	3.16	8.14	3.22	2.77
	56.51	1.22	16.16	11.15	0.24	2.56	7.62	1.93	2.47
	56.76	1.01	16.49	10.18	0	2.92	7.79	1.46	3.39
	56.76	1.05	15.98	10.25	0.26	2.79	7.63	1.74	3.36
	56.86	0.94	16.54	10.32	0	2.54	7.87	1.52	3.41
	57.01	0.99	17.19	9.62	0	2.58	7.75	1.60	3.26
	58.14	0.99	16.45	9.05	0.23	2.41	7.52	1.75	3.47
AWI7B	58.36	1.28	16.97	9.62	0.21	1.73	5.04	2.78	3.95
	58.46	1.19	16.16	10.21	0	2.49	5.28	2.96	3.25
	61.09	1.28	15.19	9.09	0.27	1.47	5.36	2.54	3.61
	62.70	0.91	15.82	7.55	0	0.71	4.45	4.00	3.68
	66.26	1.25	15.03	4.65	0	0	3.26	4.90	4.47
	66.52	1.14	15.54	4.03	0	0	3.77	3.81	4.96
AWI8	54.10	1.57	16.25	11.44	0.31	3.55	8.46	0.80	3.54
	54.41	1.61	16.05	11.22	0.24	3.43	8.52	0.82	3.70
	54.49	1.68	16.04	11.36	0.39	3.37	8.47	0.80	3.41
	54.62	1.52	16.46	11.01	0.34	3.19	8.44	0.71	3.59
	54.72	1.46	16.34	11.41	0.27	3.45	8.14	0.81	3.28
	54.82	1.55	16.31	10.94	0.33	3.23	8.19	0.80	3.76
	55.30	1.53	16.24	10.96	0.23	3.37	8.03	0.77	3.50
	55.65	1.58	16.25	10.60	0.22	3.13	7.86	0.97	3.68
	56.64	1.68	15.97	10.13	0.29	2.92	7.58	0.94	3.74
	57.70	1.60	15.87	9.59	0.26	2.78	7.12	0.86	4.22
	58.14	1.54	15.95	9.57	0.32	2.55	7.15	0.87	3.85
	58.59	1.55	16.30	9.59	0.18	2.46	6.72	0.86	3.75
	59.59	1.71	15.92	8.46	0.29	2.04	6.27	1.05	4.55
	60.25	1.30	16.04	8.64	0.21	2.32	6.31	1.00	3.85
	61.33	1.62	15.79	7.71	0.27	1.68	5.82	1.16	4.48
	62.08	1.40	15.65	8.04	0.20	1.67	5.62	1.20	4.05
	63.19	1.32	15.65	7.48	0.34	0.79	5.16	1.36	4.58
	63.71	1.28	15.43	7.05	0.24	1.10	4.81	1.41	4.88
	64.07	1.14	15.20	6.90	0.27	0.87	4.73	1.41	5.30
	64.18	1.31	15.56	6.55	0.28	1.19	4.86	1.47	4.50
	64.22	1.15	15.29	7.28	0.32	0.87	4.85	1.47	4.44
	68.07	0.93	14.50	5.55	0.26	0	3.49	1.82	5.20
Leg 113									
AWI9	57.00	1.82	15.85	9.53	0.32	2.99	6.20	1.53	4.67
	57.58	1.37	16.80	8.32	0	2.85	6.91	1.12	5.01
	58.94	1.56	17.31	7.86	0.20	1.24	5.92	1.44	5.40
	58.97	1.38	16.23	8.05	0.18	2.31	6.12	1.43	5.34
	59.18	1.53	16.22	8.24	0.28	2.23	5.85	1.48	4.95
	60.01	1.52	17.68	6.44	0	1.10	5.89	1.62	5.54
	60.56	1.19	16.92	7.29	0	1.46	5.71	1.87	4.91
	61.18	1.27	17.66	6.06	0	1.06	5.73	1.67	5.23
	61.24	1.22	17.33	6.71	0	1.14	5.05	1.57	5.68
	61.95	1.09	16.43	6.36	0.20	1.15	4.72	2.27	5.73
	62.67	1.26	16.44	6.94	0	0.94	4.45	1.96	5.25
	65.39	0.95	15.93	5.77	0	0.52	3.66	2.33	5.21
	65.59	0.58	16.94	5.05	0	0	3.45	1.96	6.36
	65.66	0.91	16.06	5.14	0.16	0.32	3.13	2.17	6.33
	65.67	0.81	16.14	5.52	0	0.34	2.95	2.12	6.33
	66.04	0.88	15.93	5.44	0.24	0	2.99	2.33	6.04
	66.21	0.66	17.09	4.35	0	0	3.18	2.16	6.27
	66.75	0.86	15.55	5.40	0	0	2.89	2.67	5.63
	66.79	0.67	15.78	5.25	0	0	2.58	2.35	6.44
	67.46	0.82	15.31	5.04	0	0	2.61	2.92	5.56
	69.42	0.57	15.56	3.33	0	0	2.06	3.08	5.87
	69.59	0.39	14.60	4.64	0	0	2.02	3.34	5.17
	69.60	0.53	14.59	4.54	0	0	1.83	3.37	5.46
AWI10	59.30	1.58	15.99	8.64	0.17	1.75	5.76	2.17	4.51
	59.47	1.43	16.23	8.69	0.21	1.73	5.68	2.14	4.35
	59.57	1.30	16.48	8.10	0	1.80	5.76	1.93	5.07
	59.66	1.49	16.15	8.14	0.22	1.86	5.84	2.02	4.47
	59.77	1.32	16.29	8.09	0.20	1.69	5.45	1.68	5.52
	59.77	1.42	15.44	8.45	0.23	2.20	5.47	2.19	4.65
	59.94	1.46	15.91	8.85	0.16	1.63	5.68	2.13	4.15
	59.96	1.15	17.07	7.37	0.15	1.39	5.93	2.09	4.76

Appendix (continued).

Sample	SiO_2 (%)	TiO_2 (%)	Al_2O_3 (%)	FeO (%)	MnO (%)	MgO (%)	CaO (%)	K_2O (%)	Na_2O (%)
	59.97	1.40	15.80	8.59	0.16	1.56	5.78	2.22	4.37
	60.08	1.28	16.91	7.86	0	1.68	5.58	1.74	4.88
	60.11	1.42	16.01	7.86	0.24	1.81	5.25	1.94	5.28
	60.23	1.55	15.71	8.35	0.30	1.56	5.36	2.21	4.63
	60.35	1.47	16.06	8.14	0.20	1.61	5.44	2.37	4.28
	60.39	1.32	15.95	8.05	0	1.85	5.40	1.90	5.06
	60.39	1.33	16.71	7.50	0.21	1.59	5.40	1.84	4.97
	60.65	1.47	16.40	7.79	0	1.32	5.45	2.28	4.58
	60.67	1.38	16.42	7.94	0	1.38	5.41	2.28	4.40
	61.05	1.35	16.26	7.46	0.20	1.67	5.21	1.96	4.85
	61.13	1.45	16.17	7.60	0.19	0.84	5.48	2.29	4.77
AWI11A	55.43	1.63	16.49	10.01	0.18	3.17	7.85	1.45	3.73
	55.45	1.70	16.52	10.19	0	2.95	7.74	1.45	3.90
	55.53	1.47	16.75	10.20	0.16	3.11	7.27	1.20	4.30
	55.71	1.61	16.61	10.05	0.26	2.94	7.81	1.42	3.57
	55.95	1.48	17.26	9.29	0.26	2.67	7.69	1.45	3.86
	55.99	1.48	16.79	9.37	0.18	2.85	7.36	1.35	4.63
	55.99	1.54	16.81	9.46	0.19	3.25	7.51	1.28	3.97
	56.36	1.31	17.56	8.48	0.37	2.65	7.25	1.42	4.60
	56.40	1.39	16.44	9.43	0.30	3.17	7.38	1.18	4.31
	56.47	1.44	17.16	8.89	0.22	2.76	7.51	1.26	4.30
	57.09	1.36	17.79	8.53	0.17	2.13	7.09	1.37	4.38
	57.88	1.28	16.97	8.69	0	2.41	6.85	1.54	4.36
	58.35	1.19	17.67	8.01	0.16	2.17	7.18	1.36	3.90
AWI11B	69.80	0.42	14.50	3.82	0.32	0	1.54	4.44	4.93
	69.89	0.27	14.77	4.12	0	0	1.96	3.62	5.16
	69.89	0.41	14.61	3.75	0.18	0	1.63	3.64	5.68
	69.99	0.44	14.31	4.02	0.20	0	1.67	4.21	4.91
	70.20	0.48	14.59	4.04	0	0	1.62	4.01	4.86
	70.29	0.32	14.40	3.90	0.16	0	1.64	4.05	4.98
	70.53	0.22	14.70	3.68	0	0	1.50	3.89	5.28
	70.66	0.29	14.56	3.62	0	0	1.43	3.92	5.31
	70.67	0.40	14.56	3.74	0	0	1.47	3.66	5.32
	70.92	0.17	14.59	3.63	0	0	1.54	3.65	5.36
	71.72	0.21	14.48	2.91	0	0	1.26	3.72	5.48
AWI12A	54.75	1.74	16.75	10.09	0.21	2.92	7.76	1.30	4.37
	55.02	1.45	16.60	10.24	0	3.32	7.61	1.06	4.69
	55.49	1.58	17.06	9.46	0.23	3.16	7.29	1.16	4.45
	55.56	1.58	16.78	9.66	0.20	3.08	7.42	1.03	4.70
	55.58	1.65	16.38	9.73	0.35	2.84	7.84	1.23	4.38
	55.86	1.69	16.21	10.54	0.24	2.83	7.30	1.56	3.70
	56.08	1.40	16.83	9.66	0	3.09	7.47	0.98	4.50
	56.53	1.50	16.66	9.41	0.31	2.76	7.34	1.38	4.03
	56.87	1.57	16.53	9.65	0	2.49	7.09	1.45	4.22
	57.68	1.56	17.03	8.48	0.20	2.41	6.95	1.33	4.26
	58.35	1.34	16.50	8.24	0.25	2.66	6.42	1.35	4.88
	58.69	1.27	16.06	8.43	0.19	2.04	6.42	1.61	5.23
	59.93	1.14	16.63	7.84	0.18	1.98	5.85	1.54	4.92
AWI12B	62.04	1.13	16.05	7.36	0.18	1.03	5.07	2.10	4.89
	63.12	1.13	16.13	7.08	0	1.40	5.15	2.22	3.55
	64.45	0.89	15.91	6.14	0	0.60	4.08	2.40	5.37
	65.06	0.91	15.90	6.28	0.19	0.64	4.22	2.49	4.06
	67.83	0.56	17.35	2.83	0	0	3.07	2.80	5.48
AWI13	56.58	1.44	16.57	9.16	0.24	2.76	6.74	1.43	4.93
	57.00	1.50	16.25	9.13	0.30	2.86	6.83	1.37	4.67
	57.21	1.47	16.02	9.74	0.27	2.54	6.96	1.50	4.11
	57.27	1.36	16.36	9.46	0	2.42	7.23	1.42	4.34
	57.35	1.48	16.56	8.75	0.28	2.70	6.64	1.30	4.78
	57.52	1.56	16.55	9.02	0.25	2.48	6.72	1.34	4.52
	57.76	1.44	16.56	9.03	0.23	2.65	6.50	1.36	4.41
	58.88	1.25	17.63	7.81	0.19	1.89	6.56	1.35	4.44
AWI14A	55.62	1.62	16.28	10.26	0.17	2.88	7.20	1.52	4.38
	55.66	1.56	16.11	10.68	0.17	3.17	7.55	1.36	3.64
	56.99	1.52	16.27	9.91	0	2.65	7.31	1.32	4.03
	57.21	1.55	15.96	9.38	0.26	2.64	7.18	1.43	4.38
	57.55	1.45	16.99	8.45	0.25	2.30	7.05	1.29	4.66
	58.03	1.51	16.43	9.31	0	2.29	6.75	1.57	4.11
AWI14B	69.66	0.34	14.57	4.15	0.18	0	1.82	3.31	5.80
	70.23	0.40	14.38	3.93	0.18	0	1.64	3.63	5.42
	70.49	0.31	14.49	4.04	0	0	1.65	3.20	5.66
	70.68	0.34	14.44	3.92	0	0	1.82	3.21	5.44
	69.66	0.34	14.57	4.15	0.18	0	1.82	3.31	5.80
	70.23	0.40	14.38	3.93	0.18	0	1.64	3.63	5.42
	70.49	0.31	14.49	4.04	0	0	1.65	3.20	5.66
	70.68	0.34	14.44	3.92	0	0	1.82	3.21	5.44
AWI15	57.46	1.16	16.50	9.09	0.32	2.72	6.61	1.37	4.60
	58.03	1.20	15.96	8.94	0.26	2.38	6.41	1.49	5.22

Appendix (continued).

Sample	SiO_2 (%)	TiO_2 (%)	Al_2O_3 (%)	FeO (%)	MnO (%)	MgO (%)	CaO (%)	K_2O (%)	Na_2O (%)
	59.06	1.10	15.88	9.09	0.26	2.33	5.88	1.55	4.75
	59.21	1.17	16.38	8.80	0.16	2.19	6.01	1.55	4.47
	59.29	1.12	16.60	8.45	0.18	2.15	5.98	1.45	4.78
	59.45	1.26	15.42	9.73	0.20	1.95	6.16	1.88	3.84
	59.78	1.05	16.03	8.69	0.29	2.31	5.97	1.56	4.24
	59.99	1.11	16.52	8.48	0.26	1.89	5.61	1.65	4.50
	60.75	1.26	15.76	8.19	0.23	1.69	5.43	2.02	4.56
	61.79	1.14	15.58	7.98	0	1.52	4.48	1.95	5.46
AWI16	54.50	1.53	16.43	10.46	0.33	3.45	8.35	1.24	3.62
	54.62	1.56	16.32	10.54	0.21	3.59	8.33	1.21	3.53
	54.73	1.35	16.53	10.02	0.25	3.70	7.89	1.05	4.50
	54.81	1.36	16.57	10.13	0.16	3.47	7.82	1.08	4.60
	54.93	1.36	16.60	9.98	0.23	3.64	7.97	1.08	4.20
	54.95	1.47	16.72	10.27	0	3.47	8.09	1.01	4.02
	54.99	1.46	16.82	10.08	0.25	3.58	7.95	1.01	3.86
	55.08	1.42	16.51	10.19	0.18	3.44	8.09	0.99	4.10
	55.08	1.55	16.27	10.20	0	3.29	8.34	1.21	4.06
	55.37	1.33	16.41	10.32	0	3.31	8.09	1.01	4.16
	55.83	1.38	16.65	9.74	0	3.42	7.80	1.03	4.16
	56.18	1.45	16.68	9.49	0.23	3.11	7.87	1.37	3.56
AWI17	53.91	1.15	16.12	9.61	0	4.93	10.07	1.07	3.14
	54.64	1.03	16.57	8.72	0.23	4.65	9.18	1.11	3.88
	56.42	0.98	17.33	8.57	0.22	3.35	7.22	1.11	4.71
	57.07	1.01	16.81	8.79	0.19	2.99	7.18	1.19	4.78
	58.21	1.42	16.02	8.95	0.26	2.21	6.21	1.38	5.29
	58.30	1.49	16.15	8.90	0.22	2.36	6.20	1.42	4.96
	58.36	1.33	16.29	8.73	0.24	2.28	6.03	1.46	5.16
	58.37	1.39	16.19	8.85	0.18	2.53	6.04	1.43	5.01
	58.59	1.43	16.49	8.48	0.23	2.25	5.99	1.46	5.09
	58.66	1.40	16.34	8.82	0.24	2.36	6.22	1.33	4.62
	58.83	1.50	16.38	8.76	0	2.17	5.89	1.57	4.83
	59.17	0.84	16.43	8.07	0.17	2.50	6.28	1.48	4.97
	59.83	1.23	15.99	8.49	0.18	1.86	5.50	1.72	5.20
	62.30	1.27	16.30	7.00	0.21	0.95	4.22	2.39	5.21
	63.94	1.07	17.15	5.61	0	0.22	4.57	2.37	4.95
	67.11	0.55	15.15	5.67	0.16	0	2.68	2.45	6.13
	67.96	0.64	15.17	5.34	0.21	0	2.46	2.51	5.65
	71.34	0.35	14.64	3.42	0	0	1.40	3.37	5.35
AWI18	57.92	1.77	15.18	10.4	0.16	2.25	6.15	1.55	4.61
	58.11	1.51	15.98	9.32	0.16	2.29	6.56	1.28	4.80
	58.27	1.57	16.01	9.35	0.33	2.00	6.44	1.60	4.30
	58.69	1.34	16.00	8.97	0	2.29	6.02	1.30	5.33
	58.77	1.21	16.63	8.34	0.32	2.02	6.07	1.25	5.28
	59.17	1.38	15.95	9.02	0.17	2.14	5.62	1.40	5.16
	59.40	1.51	15.91	8.73	0.19	2.10	5.86	1.37	4.85
	59.71	1.37	15.92	8.53	0.30	1.91	5.46	1.54	5.17
	59.91	1.42	16.26	7.96	0.28	1.81	5.65	1.53	5.12
	60.54	1.10	16.46	7.38	0.29	1.43	5.90	2.00	4.90
	61.25	1.32	16.52	7.46	0.17	1.00	5.27	1.99	4.96
	62.70	0.90	17.21	5.75	0	0.58	5.09	1.99	5.66
AWI19	57.65	1.18	16.62	9.06	0.26	2.49	6.96	1.43	4.25
	57.93	1.24	16.80	8.36	0.33	2.44	6.68	1.65	4.46
	58.78	1.22	16.64	8.32	0.26	2.15	6.43	1.72	4.38
	59.41	1.19	16.26	8.15	0.22	1.84	5.90	1.98	4.86
	60.50	1.13	16.06	7.58	0.34	1.66	5.53	2.07	4.98
	60.63	1.07	15.91	8.10	0.27	1.74	5.65	1.97	4.49
	60.96	1.17	16.08	7.68	0.23	1.78	5.55	2.02	4.26
	61.15	1.04	16.06	7.67	0.23	1.64	5.41	2.06	4.59
	61.35	1.01	15.95	7.63	0.22	1.58	5.44	2.02	4.63
	61.38	1.21	15.76	7.65	0.25	1.23	5.23	2.18	5.03
	61.92	1.07	15.81	7.24	0.23	1.28	5.30	2.17	4.81
	62.62	0.97	16.25	6.67	0.32	1.27	4.67	2.23	4.82
	63.13	1.10	15.08	7.55	0.24	1.06	4.19	2.49	4.98
	63.26	1.01	14.36	7.96	0.19	1.67	5.98	1.48	3.97
	63.99	0.90	15.81	6.67	0.20	0.73	4.18	2.39	4.98
	64.20	0.84	15.66	6.37	0	0.90	4.36	2.38	5.10
	64.29	0.88	15.74	6.30	0.30	0.72	4.14	2.42	5.02
AWI20	58.66	1.33	15.97	9.26	0	2.04	6.27	2.08	4.29
	59.99	1.26	16.22	8.52	0.17	1.48	6.02	2.07	4.17
	60.30	1.38	15.62	8.31	0.25	1.73	5.42	2.27	4.59
	60.45	1.36	15.92	8.18	0.18	1.72	5.50	2.19	4.37
	60.78	1.48	15.70	7.82	0.22	1.75	5.30	2.26	4.51
	60.84	1.21	16.20	7.40	0.28	1.34	5.33	2.20	5.06
	61.16	1.20	16.06	7.70	0.24	1.41	5.35	2.27	4.48
	61.26	1.28	16.06	7.80	0.26	1.49	5.00	2.37	4.33
	61.90	1.10	15.70	7.61	0.29	1.29	4.79	2.44	4.71
	62.12	1.19	15.63	7.31	0.25	1.21	4.79	2.47	4.84
	62.53	1.06	15.84	7.32	0	1.20	4.61	2.50	4.77

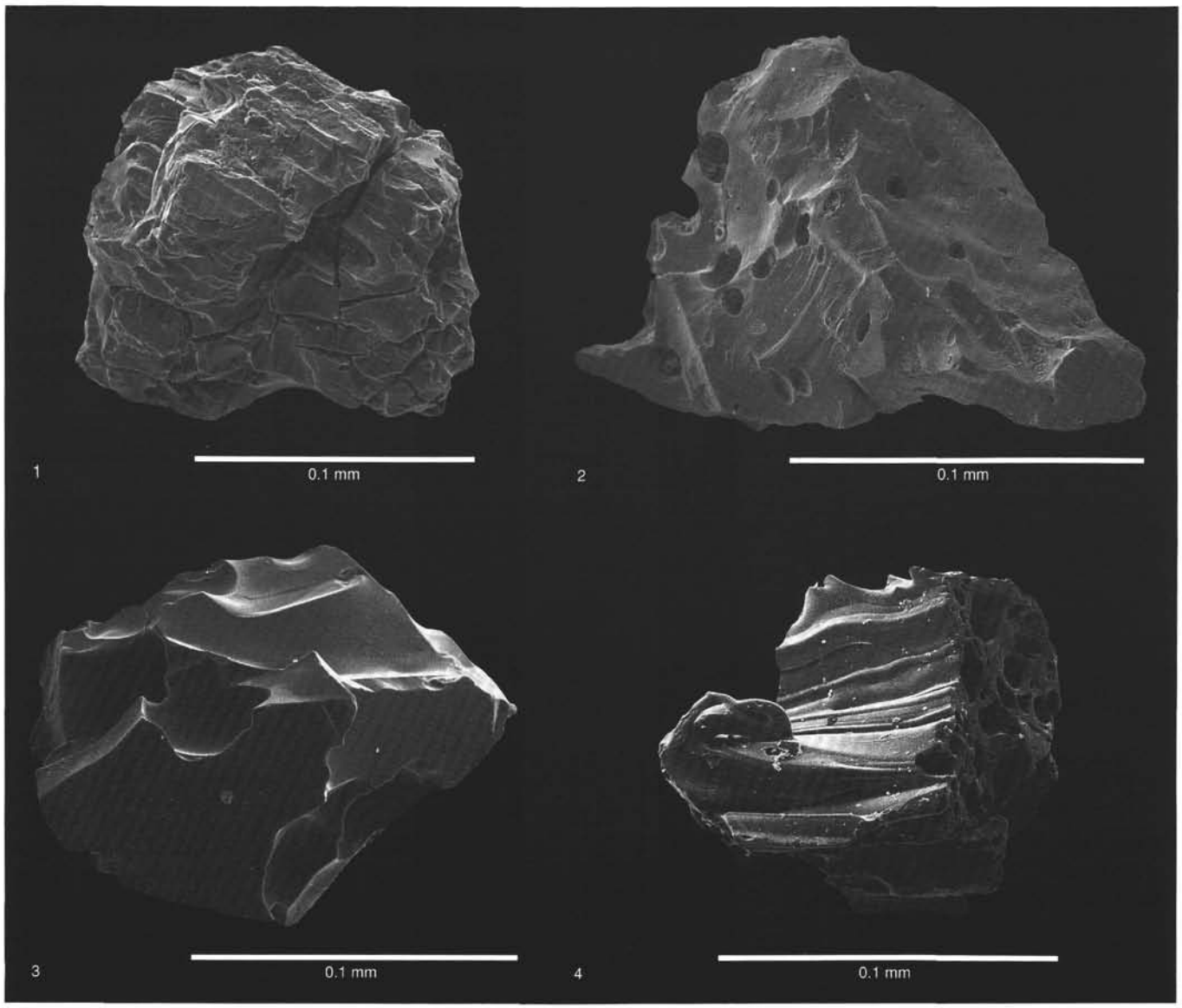

Plate 1. SEM images of glass shards from Site 701, showing observed variability of shard morphology in all samples investigated. Bar = 0.1 mm. **1.** Equant, blocky-shaped grain with no vesicles. The cracks are presumably due to shock cooling in contact with water or ice. **2** and **3.** Shattered, equant, blocky grains with low to medium vesicularity. **4.** Highly vesicular, strongly elongated, tubular structures caused by a high eruption rate. The bubble caves are partly collapsed or deformed.

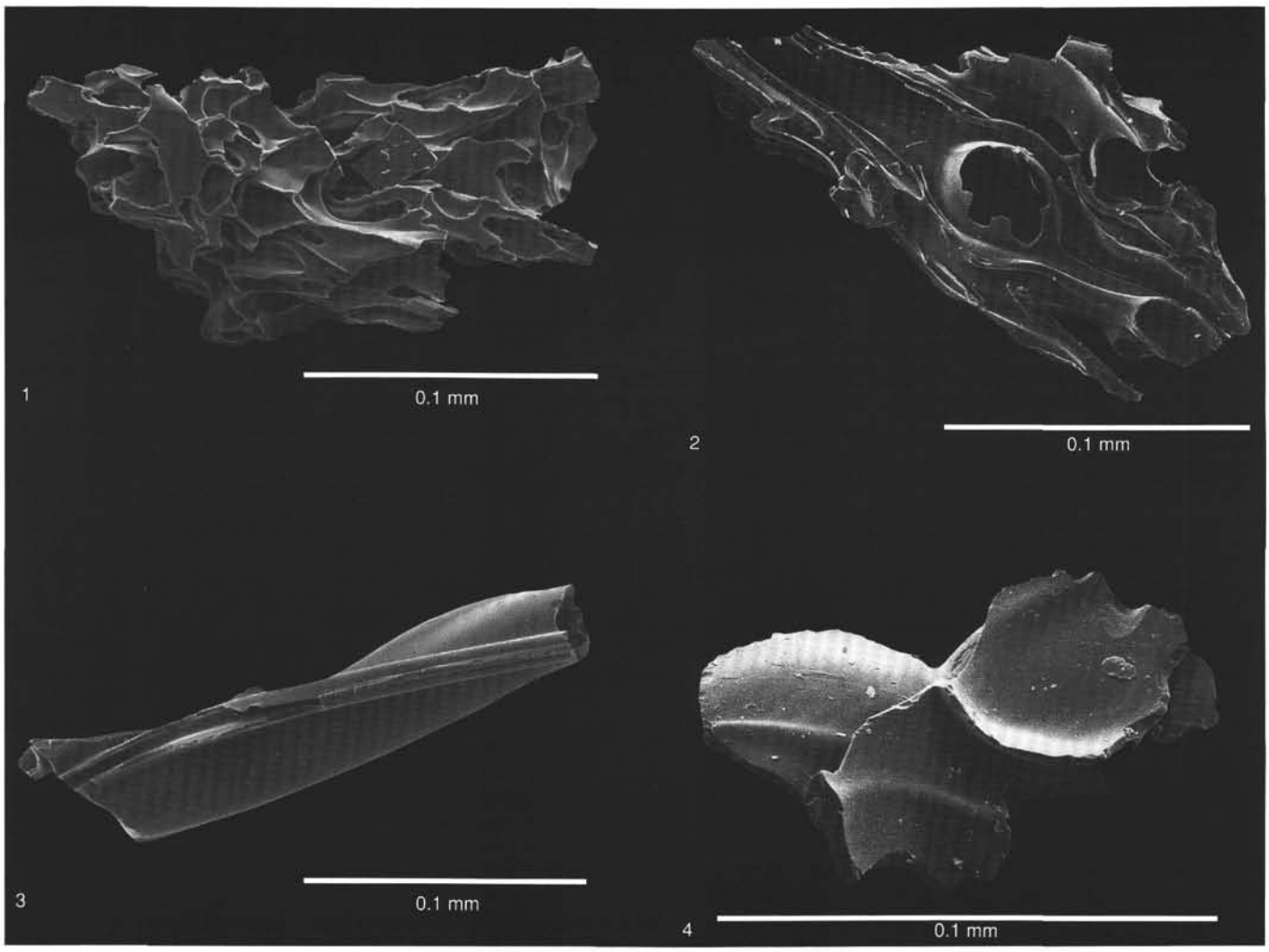

Plate 2. SEM images of glass shards from Site 701, showing observed variability of shard morphology in all samples investigated. Bar = 0.1 mm. **1.** Very strongly vesicular, pumiceous particle with typical Y-shaped vesicle junctions, indicating low viscosity and/or high volatile contents of the magma. **2.** Strongly elongated, fibrous structure with delicate collapsed bubble walls. **3.** Fragment of extremely elongated bubble cavities, with a very low width/length ratio. **4.** Platy to cuspate structures caused by fragmentation of bubble walls.